HHS Public Access

Author manuscript

J Magn Reson Imaging. Author manuscript; available in PMC 2023 July 06.

Published in final edited form as:

J Magn Reson Imaging. 2023 July ; 58(1): 44–60. doi:10.1002/jmri.28689.

Updates on Compositional MRI Mapping of the Cartilage: Emerging Techniques and Applications

Marcelo V. W. Zibetti, PhD[*],
Rajiv G. Menon, PhD,
Hector L. de Moura, PhD,
Xiaoxia Zhang, PhD,
Richard Kijowski, MD,
Ravinder R. Regatte, PhD

Center of Biomedical Imaging, Department of Radiology, New York University Grossman School of Medicine, New York, New York, USA

Abstract

Osteoarthritis (OA) is a widely occurring degenerative joint disease that is severely debilitating and causes significant socioeconomic burdens to society. Magnetic resonance imaging (MRI) is the preferred imaging modality for the morphological evaluation of cartilage due to its excellent soft tissue contrast and high spatial resolution. However, its utilization typically involves subjective qualitative assessment of cartilage. Compositional MRI, which refers to the quantitative characterization of cartilage using a variety of MRI methods, can provide important information regarding underlying compositional and ultrastructural changes that occur during early OA. Cartilage compositional MRI could serve as early imaging biomarkers for the objective evaluation of cartilage and help drive diagnostics, disease characterization, and response to novel therapies. This review will summarize current and ongoing state-of-the-art cartilage compositional MRI techniques and highlight emerging methods for cartilage compositional MRI including MR fingerprinting, compressed sensing, multi-exponential relaxometry, improved and robust radio-frequency pulse sequences, and deep learning-based acquisition, reconstruction, and segmentation. The review will also briefly discuss the current challenges and future directions for adopting these emerging cartilage compositional MRI techniques for use in clinical practice and translational OA research studies.

Quantitative cartilage compositional mapping is an important emerging topic in musculoskeletal imaging, particularly due to its potential for early diagnosis of osteoarthritis (OA) and subsequent monitoring of disease progression.[1] OA is a chronic and debilitating musculoskeletal disease causing progressive and irreversible degeneration of cartilage and other joint structures. OA currently affects over 27 million people in the United States alone and has a worse outlook in the years ahead due to the aging population and the current obesity epidemic.[1,2] The diagnosis of OA is made based on clinical symptoms such

[*]Address reprint requests to: M.V.W.Z., Department of Radiology, New York University Grossman School of Medicine, 660 First Avenue, 4th Floor, New York, New York, USA. marcelo.wustzibetti@nyulangone.org.

as joint pain and stiffness and the presence of definitive osteophytes on radiographs, with secondary findings of joint space narrowing (JSN) considered a surrogate marker of disease progression.[3]

Articular cartilage is mainly composed of water, which comprises 65%–85% of its net weight, and an abundant extracellular matrix (ECM) consisting of predominantly type II collagen fibers and large proteoglycan (PG) macromolecules.[4] PG contains long glycosaminoglycan (GAG) side chains with negatively charged sulfate and hydroxyl groups that create a fixed charge density (FCD). The negative FCD attracts cations such as sodium that result in osmotic pressure that draws water into the cartilage.[5] This produces a swelling pressure built up by the electrostatic repulsion between the GAG side chains in the cartilage ECM, which provides the underlying viscoelastic properties necessary for load distribution. The swelling pressure is constrained by the collagen fiber network, which provides the tensile force opposing the expansion of cartilage.[4] Early OA is primarily characterized by a loss of PG, followed by the subsequent decrease in water content due to the reduction of osmotic pressure.[5]

Magnetic resonance imaging (MRI) is uniquely suited for characterizing human articular cartilage, providing both morphological and compositional evaluation.[6] Compositional MRI is especially useful as it can detect changes in the composition and ultrastructure of cartilage during the earliest stages of cartilage degeneration before the onset of morphological cartilage loss. Compositional MRI can also monitor disease- and treatment-related changes in cartilage composition and ultrastructure over time in clinical practice and longitudinal OA research studies. Compositional MRI techniques are effective in evaluating cartilage in a variety of joints including the knee, hip, and ankle.[7–9]

In this review article, section “Summary of current methods used for compositional MRI of cartilage” summarizes the current state-of-the-art cartilage compositional MRI techniques as well as some recent methods for cartilage morphometry that have been used in clinical practice and OA research studies. Methods described include T_2 and T_2^* mapping, $T_{1\rho}$ mapping, T_1 mapping with gadolinium contrast, ultrashort echo time (UTE) imaging, chemical exchange saturation transfer (gagCEST) imaging, sodium imaging, diffusion imaging, and morphometry (Table 1). Section “Emerging methods for quantitative MRI for cartilage” highlights emerging methods for cartilage compositional MRI including MR fingerprinting (MRF), compressed sensing (CS), multiexponential relaxometry, improved and robust radio-frequency (RF) pulse sequences, and deep learning (DL)-based acquisition, reconstruction, segmentation methods and MRI based biomechanical assessment. Finally, section “Summary of discussion and future directions” will briefly discuss the current challenges and future directions for adopting these emerging cartilage compositional MRI techniques for use in clinical practice and translational OA research studies.

Summary of Current Methods Used for Compositional MRI of Cartilage

T_2 Mapping

T_2 mapping is a quantitative MRI method that serves as a surrogate marker for water content and collagen structure. The T_2 relaxation time of cartilage primarily provides information

regarding collagen fiber orientation and the integrity of the collagen fiber network.[10] While increased hydration of cartilage should theoretically lead to an increase in T_2 relaxation time, not all studies have shown a direct correlation between T_2 relaxation time and the water content of ex vivo cartilage samples.[11] In healthy cartilage, the water content is high, but water is tightly bound to the hydrophilic GAG side chains of PG. With cartilage degeneration, there is a disorganization of the collagen fiber network and a decrease in proteoglycan content resulting in the presence of more unbound, freely mobile water. T_2 relaxation time measurements increase with the unbound water content, which enables T_2 mapping to pick up early signs of cartilage degeneration in OA that may not be apparent on morphological imaging sequences.[12]

T_2 mapping is typically performed with a range of echo times using 2D or 3D multiecho spin echo sequences or T_2 preparation modules, combined with later data fitting using mono-exponential models. More recently, 3D double-echo steady-state (DESS) sequences are used, which allows the joining quantification of T_1 relaxation and apparent diffusion coefficient (ADC) in addition to T_2 relaxation time.[13] The main advantage of T_2 mapping is the commercial availability of T_2 pulse sequences on most MRI vendor platforms. Acknowledged drawbacks of T_2 mapping include long acquisition times, stimulated echoes, susceptibility to magic angle effects, imperfect RF pulses, reduced sensitivity to PG, magnetization transfer effects, and offline reconstruction methods.[12]

T_2^* Mapping

Similar to T_2, the T_2^* mapping is also a surrogate marker for water content and collagen structure.[14] However, T_2^* is also influenced by coherent dephasing effects due to local magnetic field in-homogeneities. T_2^* mapping is usually performed with fast gradient recalled echo (GRE) sequences, and, due to de-phasing, T_2^* values are usually shorter than T_2. T_2^* mapping offers the advantages of fast imaging, 3D acquisition, and high spatial resolution, with no additional hardware or special sequences required. T_2^* studies have shown good reproducibility.[6,14,15]

T_2^* mapping offers unique information useful for the characterization of cartilage. T_2^* contrast captures shorter decay times in the cartilage and is less sensitive to bulk water. Decreases in T_2^* values are reported in deeper layers of normal cartilage and increased T_2^* values in pathology.[16,17] T_2^* mapping combined with UTE sequences have been useful to characterize calcified cartilage with decay times lower than 1 millisecond (msec).[18]

$T_{1\rho}$ Mapping

$T_{1\rho}$ mapping is an endogenous contrast technique that is sensitive to the GAG content of cartilage.[19,20] The exchange of protons between water and the hydroxyl and amine groups on the GAG side chains of PG is thought to be the primary mechanism for $T_{1\rho}$ dispersion within cartilage.[21] A strong correlation has been found between cartilage $T_{1\rho}$ relaxation time and FCD.[22] The reduction of GAG content within cartilage has also been shown to increase cartilage $T_{1\rho}$ relaxation times in in vitro and ex vivo studies.[23,24] However, $T_{1\rho}$ relaxation time is not a specific measure of the GAG content of cartilage and is also

influenced by other biological changes that occur with cartilage degeneration.[25] Although T_2 and $T_{1\rho}$ relaxation time values are correlated, it has been shown that $T_{1\rho}$ relaxation time is more sensitive than T_2 relaxation time for detecting early cartilage degeneration in human subjects.[26]

$T_{1\rho}$ mapping is performed by applying a preparatory spin-lock pulse (SLP) after the magnetization is tipped onto the transverse plane. The signal is then allowed to decay under the presence of the SLP, with the $T_{1\rho}$. $T_{1\rho}$ contrast is sensitive to the kilohertz range because of the reliance on the RF-generated B_1 field. This makes the $T_{1\rho}$ signal sensitive to chemical exchange between macromolecules and bulk water.[25] The advantages of $T_{1\rho}$ mapping are that $T_{1\rho}$ dispersion is sensitive to PG loss in cartilage, provide cartilage-specific underlying mechanisms, and are not as strongly influenced by magic angle effects as T_2 mapping. Some of the drawbacks of $T_{1\rho}$ mapping include its long scan times, relatively high specific absorption rate (SAR) during the $T_{1\rho}$ preparation pulses and the need for customized RF pulse sequences.

T_1 Mapping and dGEMRIC

T_1 mapping for cartilage applications[27] usually uses a contrast-based method called delayed gadolinium-enhanced MRI of cartilage (dGEMRIC). dGEMRIC employs a negatively charged gadolinium contrast agent to adhere to the negative FCD of GAG side chains of PG. GAGs repel the contrast agent and its distribution is mapped in inverse proportion to local PG content, with a higher concentration of contrast agent where GAG concentration is low. The higher concentration of contrast agent will reduce T_1 relaxation times in areas of low GAG concentration. The T_1 relaxation time of native and enzymatically degraded ex vivo cartilage samples in the presence of gadolinium contrast has been found to strongly correlate with the PG content[28] and compressive stiffness of cartilage.[29]

The dGEMRIC technique has been shown to detect surgically and histologically confirmed early cartilage degeneration in human subjects due to its sensitivity and specificity to PG content and FCD.[30] However, challenges in the clinical adoption of dGEMRIC have limited its widespread use. Some of the challenges are that the technique uses exogenous contrast agent injections that may cause nephrogenic systemic fibrosis and gadolinium deposition in tissues, lack of standardization of dGEMRIC protocols, and the long wait time following contrast administration depending on the cartilage anatomy and thickness. The use of ionic vs. nonionic contrast agents has also been debated with varying results.[27]

UTE MRI

UTE imaging allows the characterization of semi-solid tissues with highly organized collagen fibers and very short relaxation times including the menisci, tendons, ligaments, and deep calcified layers of cartilage, which appear dark on typical MR images due to signal loss. UTE techniques can be used to measure T_1, T_2, T_2^*, and $T_{1\rho}$ relaxation times of the tissue of interest. However, UTE imaging assesses effective relaxation times and is also influenced by tissue susceptibility and magnetic field inhomogeneity.[31]

To achieve UTE imaging to characterize rapidly decaying signals, gradient echo sequences are used with half-excitation RF pulses in the 0.05–0.2 millisecond range.[31] More recent work described a pointwise encoding time reduction with radial acquisition (PETRA) sequence for UTE imaging, which used combined Cartesian and radial imaging to achieve short TE and longer TE, to visualize all fast and slow decaying structures together.[32] With UTE imaging, there are challenges with off-resonance, radial trajectory errors, and distortion of slice profile, but these can be addressed with off-resonance correction, gradient trajectory calibration, and efficient fat suppression.

gagCEST MRI

GAG chemical exchange saturation transfer (gagCEST) is a magnetization transfer contrast technique that uses off-resonance pulses to saturate exchangeable labile protons in the GAG side chains of PG.[33] A gagCEST technique at 3 T is comparable to dGEMRIC and T_2 mapping for characterizing degenerative cartilage.[34] A strong correlation between gagCEST and sodium values within both healthy cartilage and cartilage repair tissue has also been reported, which suggests that gagCEST can be used to assess the FCD of cartilage.[33] While gagCEST imaging is a potentially powerful technique for evaluating PG within cartilage, clinical studies exploring the feasibility of early OA detection are still limited due to the small contrast changes between normal and degenerative cartilage that occur on clinical 3 T scanners.

To perform gagCEST imaging, a spoiled gradient-echo sequence is used with a range of off-resonance saturation pulses applied to directly saturate water protons associated with the macromolecules. Although gagCEST provides sensitive and specific information regarding PG in cartilage, the technique has several drawbacks. These include low SNR on systems below 7 T, thus requiring ultra-high field systems for scanning, the need for customized RF pulse sequences, long RF pulses for off-resonance saturation leading to high RF energy deposition, and complex postprocessing techniques.[33,34]

Sodium MRI

The sodium ion (^{23}Na) possesses a quadrupolar moment that interacts with electric field gradients. Sodium reacts to the FCD in cartilage and can be used as a biomarker for GAG content. Clinical validation is limited in the literature, in part due to the challenges associated with sodium imaging. Sodium imaging has been used to compare cartilage in healthy subjects and subjects with early OA, reporting higher FCD in healthy individuals.[35] High reproducibility and repeatability of sodium quantification in the cartilage at 3 T and 7 T field strengths have been reported.[36] Sodium imaging has been used to evaluate cartilage repair following surgery.[37] Multinuclear, dual-tuned sodium and proton RF coils for specific use in the knee have also been developed, which allow combined sodium and morphological imaging of cartilage.[38]

The sodium concentration of healthy cartilage is 200–300 mmol/L, which is about 260–400 times lower than the proton concentration. This dramatically reduces the signal available and requires longer scan times or the use of higher magnetic fields to improve SNR.[35,36] Sodium imaging also requires specialized RF coils and customized UTE sequences to detect

signals.[38] Despite these challenges, sodium MRI has the potential to be used as a sensitive and specific biomarker for GAG to quantitatively characterize the FCD of cartilage.

Diffusion MRI

Diffusion imaging has long been used for brain imaging in focal ischemia, as a marker for restricted diffusion. More recently, diffusion imaging has been applied to cartilage imaging applications. The apparent diffusion coefficient (ADC) can be used as a measure of the interaction of water with the surrounding macromolecular matrix. Fractional anisotropy (FA) allows the determination of the main direction of local diffusion of water protons. Studies using enzymatic degradation of ex vivo cartilage specimens have shown changes in ADC with PG depletion[39] and changes in both ADC and FA with collagen depletion.[40] FA has been found to correlate strongly with the orientation of the collagen fiber network of cartilage assessed using polarized light microscopy.[41] ADC and FA have also been shown to be highly sensitive for detecting early cartilage degeneration in both ex vivo[42] and in vivo[43] studies.

To perform diffusion-weighted imaging (DWI) in musculoskeletal applications, pulse sequences with steady precession (DW-FISP) are most commonly used.[44] The diffusion-weighted double echo steady-state free precession (SSFP) has also been used for quantitative in-vivo diffusion imaging.[45] Although it is a potentially powerful technique for evaluating both PG and collagen within cartilage, significant challenges remain in using diffusion imaging including sensitivity to motion, long scan times, and limited SNR.

Quantitative Morphometry

Morphological changes in cartilage in OA can also be quantitatively assessed by segmenting and measuring the segmented cartilage, in a process known as cartilage morphometry.[46] It usually requires high-resolution 3D sequences with sufficient contrast between cartilage and surrounding tissues, assessing morphological features such as cartilage area, volume, and thickness. Cartilage morphometry has shown great repeatability.[46] Also, morphometry with DL is an interesting approach to evaluating the loss of cartilage in longitudinal studies.[47] Despite these advantages, morphometry cannot assess premorphological changes in the cartilage ECM compared to most quantitative compositional MRI methods.

Emerging Methods for Quantitative MRI for Cartilage

Search Methodology

This section will discuss the emerging methods for quantitative MRI for cartilage. Reviewed papers were selected from Google Scholar and PubMed, searching for the words: “quantitative,” “MRI,” and “cartilage,” between 2020 and 2023. To reduce overlap with recent review articles on rapid knee MRI[48] and DL methods for fast imaging and relaxometry,[49,50] some references already in these reviews may not be cited here. This section provides an update on the newly emerging techniques described after the ones cited in these previously published review articles.

Updates on Accelerated MRI Using CS and DL for Reconstruction and Direct Quantitative Mapping

Rapid acquisition for quantitative MRI mapping techniques is fundamentally important to obtain information regarding cartilage composition and ultrastructure in clinically feasible scan times. Shortening scan time for quantitative MRI mapping techniques while maintaining high-spatial resolution has several advantages including reduced healthcare costs, increased patient comfort, and decreased motion artifacts. Undersampling k-space acquisitions, followed by advanced reconstructions such as CS or DL to remove aliasing artifacts, can achieve reduced scan time, which is known as accelerated MRI.

Model-based and CS reconstructions are still active research topics for accelerating cartilage compositional MRI techniques. In the literature,[51] a CS reconstruction using robust tensor principal component analysis (PCA) models was proposed to accelerate cartilage $T_{1\rho}$ mapping, showing good agreement of $T_{1\rho}$ values between CS and fully sampled (FS) acquisitions. A model-based acceleration for diffusion imaging was proposed for musculoskeletal applications, and the feasibility of acceleration factors of 3.65 was shown without compromising diffusion data fidelity.[52]

DL-based image reconstruction is currently one of the most active topics in medical imaging research. New studies have combined CS iterative methods with DL models, such as in the literature[53] where the authors proposed a multilayer basis pursuit framework to improve knee images, showing a better peak signal-to-noise ratio than previous approaches. CS and DL reconstructions were compared for $T_{1\rho}$ mapping using mono- and bi-exponential models, where spatial and spatiotemporal priors were compared, as shown in Fig. 1.[54] Radmanesh et al[55] explored the limits of acceleration using the variational network. Different networks were trained using acceleration rates of up to 100 times. The assessments showed diagnostic quality for 2D acquisitions was obtained using an acceleration factor of $R = 4$, as shown in Fig. 2. New rapid MRI reconstruction methods have been proposed by Kim et al[56] for parallel imaging and simultaneous multislice acceleration with DL for evaluating the knee joint. The quality of the images of the proposed DL approach is equivalent to parallel MRI, but with a reduction of 71% of the acquisition time.

One of the main limitations of DL-based reconstructions is the failure to recover enough image quality to identify subtle but clinically important abnormalities, such as the meniscal tear.[57] This failure could result from the training datasets that underrepresent this subtle yet salient feature. A generative adversarial network (GAN) was proposed to improve the quality of images reconstructed by DL methods, particularly edge details.[58] It was shown that training DL methods with loss functions for a specific region of interest (ROI) could improve the performance of the DL models for that particular ROI, as shown in Fig. 3 where the ROI is the cartilage in the knee and hip.[59]

In addition to DL-based reconstruction, MRI can be accelerated in the slice direction with image super resolution. The impact of DL super resolution on MRI biomarkers of knee OA was investigated. It was found that DL super resolution could improve the quality of morphological images for detecting knee joint pathology without biasing quantitative biomarkers estimation.[60]

Large datasets may be needed for DL training. A recent public release of a knee dataset for quantitative T_2 mapping that also includes cartilage segmentation and pathology annotations could be found in.[61] Also, augmentation schemes and mixtures of FS and undersampled data for training to better utilize data in a dataset were discussed.[62,63]

Joint learning of sampling pattern (SP) and DL reconstruction was proposed in the literature.[64] The results showed that the quality of spatiotemporal undersampling could be improved by 20% or more if learned together with the DL reconstruction parameters. In Fig. 4, some results of the literature[64] illustrate how the learned SP may differ depending on the choice of DL architecture for reconstruction. Improvements can be easily seen in the joint learning approach when compared against the DL reconstruction with fixed SP, such as variable density with Poisson disc (VD + PD).

While quantitative MRI maps are usually computed from the reconstructed relaxation-weighted images, several studies have shown that it may be advantageous to compute the quantitative maps directly from k-space data or undersampled images, particularly when DL methods are used. A deep neural network for cartilage $T_{1\rho}$ and T_2 mapping was used together with spatiotemporal undersampling.[65] The results showed that it was possible to reduce the number of relaxation-weighted images from 8 to 2 (a temporal acceleration factor of $R = 4$), while also using k-space undersampling with acceleration factors of 2–6, obtaining a maximum combined spatiotemporal acceleration of $R = 24$. Similar spatiotemporal undersampling levels with neural network recovery were also demonstrated by[66] for cartilage $T_{1\rho}$ mapping.

Improved training with GANs was demonstrated in the study by Liu et al,[67] where GANs produced sharper cartilage T_2 maps. Self-supervised learning for quantitative cartilage mapping with neural networks was also proposed in the literature,[68] improving training when FS data are not available. Figure 5 shows a diagram block of the proposed method, called reference-free latent map extraction (RELAX), with some illustrative results of cartilage T_1 and T_2 maps compared to zero-fill. The results showed that no reference maps were needed for model training.

Updates on Improved RF Pulse Sequences and Sequence Optimization

Improved RF pulse sequences are essential for acquiring data efficiently. While advanced reconstruction methods can remove undersampling artifacts and other imperfections, it is ultimately the data acquisition pulse sequence that defines how long the acquisition takes and how much SNR can be obtained from a particular scan. In this sense, the accuracy and precision of the measured k-space data are extremely dependent on the chosen pulse sequence and its parameters.

Data-driven approaches based on Cramer-Rao lower bounds (CRLB) and matched sampling-fitting methods were used to optimize the spin-lock times (TSLs) in mono-exponential cartilage $T_{1\rho}$ mapping.[69] While it is known that two $T_{1\rho}$-weighted images are the minimum necessary for $T_{1\rho}$ mapping, this study showed that the right choice of the TSLs could improve image quality and parameter estimation, obtaining results better than if three or more nonoptimized TSLs were chosen. The CRLB approach to choosing the TSLs was

extended to bi-exponential and stretched-exponential $T_{1\rho}$ mapping, showing that nearly the same quality can be obtained using half of the number of TSLs if they were optimized.[70]

Efficient use of phase-cycling acquisitions in magnetization-prepared angle-modulated partitioned k-space spoiled GRE snapshots (MAPSS) sequences was proposed.[71] To reduce the T_1 contamination that affects the precision of cartilage $T_{1\rho}$ mapping, MAPSS required essentially two acquisitions with the same TSLs, one regular and the other with phase cycling. Peng et al[71] demonstrated that a new complex-valued curve-fitting model could solve the issue of T_1 contamination and acquisition time could be reduced. In the study by Han et al,[72] it was shown that MAPSS could be used efficiently to directly measure R_2–$R_{1\rho}$ maps of knee cartilage without having to acquire data to produce T_2 and $T_{1\rho}$ maps. However, the right preparation time (TSL and TE) must be chosen, as discussed in the literature.[72]

Data-driven optimized variable flip-angles (OVFA) were used to improve the accuracy and precision of magnetization-prepared spoiled gradient echo (MP-GRE) and MAPSS sequences.[73] In this study, it was demonstrated that VFA could be optimized to reduce undesired effects in the signal evolution, improving accuracy by reducing T_1 contamination and k-space filtering effects in cartilage $T_{1\rho}$ mapping, while increasing signal strength and consequently SNR. The optimized VFA could also reduce the dead time of the sequence, thereby reducing acquisition time. This is particularly important to improve the resolution of cartilage $T_{1\rho}$ maps, as shown in Fig. 6.

New spin-lock pulses for $T_{1\rho}$ mapping have been proposed in the literature[74] using adiabatic pulses, and in the studies[75,76] using self-compensated and balanced spin-lock schemes. These new preparation pulses could be used in sequences such as MAPSS and MP-GRE to improve imaging robustness due to B0 and B1 inhomogeneities.

New extensions of DESS sequences have appeared in the study by Zijlstra et al,[77] with the proposal of a new sequence called multiple-echo steady-state (MESS) to jointly produce T_2 mapping and water–fat separation with chemical-shift correction. It was shown that quantitative DESS (qDESS) could be used to measure B_0 field inhomogeneity.[78] The diagnostic quality of a 5-minute (min) sequence based on qDESS was evaluated to detect knee joint pathology, showing high interreader agreement between the new 5-minute sequence and a conventional 20-minute MRI.[60] Figure 7 illustrates some of the images obtained in the study.

Multiexponential Methods and UTE Sequences

Tissues may be composed of water in different compartments. In cartilage and other musculoskeletal tissues, there are two primary water components: fast-relaxing water tightly bound to the macromolecular matrix and slow-relaxing, freely mobile bulk water. The different water components of musculoskeletal tissues may lead to multiexponential relaxation within an image voxel. One common model to characterize multiexponential decay within a voxel is to use a two-compartment bi-exponential model. The bi-exponential models could provide better discrimination between healthy subjects and OA patients (KL-1,2) for early detection of OA, as illustrated in Fig. 8.

Most RF pulse sequences for quantitative mapping can measure tissues with relaxation times greater than 5 msec. However, some tissues in the knee joint including the deep and calcified cartilage, ligaments, tendons, and menisci have shorter T_2 relaxation times where the use of UTE or zero echo time (ZTE) sequences is needed to capture a signal.[79] This is important in clinical applications, such as OA,[80] where UTE and ZTE can better quantify the short T_2/$T_{1\rho}$ tissues such as calcified cartilage, menisci, ligaments and tendons. UTE cones and adiabatic $T_{1\rho}$ were used to assess cartilage degeneration,[81] while the study by Wu et al[82] also shows that adiabatic $T_{1\rho}$ was more robust to magic angle effects.

A stretched-exponential fitting method was described to measure T_2 and $T_{1\rho}$ relaxation of the intervertebral discs (IVD) of the spine.[83] The results demonstrated that the extra parameter of the stretched-exponential had a monotonic relationship consistent with reported variations in PG content within the IVD.

A method for rapid bi-exponential T_2^* analysis was proposed in the litertature[84] using a single scan ramped hybrid-encoding (RHE) method. The approach produced bi-exponential maps of the knee joint with a 9-minute scan time. A bi-exponential analysis of T_2^* relaxation time in the cartilage is shown in Fig. 9. A tricomponent model for T_2^* analysis of cortical bone was described, which significantly improved the estimation of bound-water and pore-water in cortical bone.[85]

MR Fingerprinting and Multicontrast Methods

Quantitative MRI mapping can reveal important information about knee joint tissues, particularly cartilage. In this sense, acquiring additional relevant parameters can provide more complementary and corroborative information. Acquiring several quantitative maps (eg T_1, T_2, and $T_{1\rho}$) separately can be very slow and inefficient. MRF[86] and multicontrast methods are efficient techniques to simultaneously estimate multiple MRI relaxation parameters. In general, they combine an improved pulse sequence with undersampling for an accelerated comprehensive multiparametric quantitative MRI mapping.

A novel MRF sequence was implemented for simultaneous T_1, T_2, and $T_{1\rho}$ relaxation mapping of the human knee joint at 3 T.[87] With the use of $T_{1\rho}$ preparation modules, the MRF sequence showed the feasibility of simultaneously estimating proton density (PD), T_1, T_2, $T_{1\rho}$, and B_1. The in vivo experiments also showed that multi-parameter cartilage relaxation time measurements from the novel MRF sequence could distinguish early OA patients from healthy subjects. The feasibility of the MRF sequence for simultaneous PD, T_1, T_2, $T_{1\rho}$, and B_1 mapping of the hip joint was further demonstrated in the literature.[88] The experiments showed excellent repeatability of PD, T_1, T_2, $T_{1\rho}$, and B_1 parameter estimations. The same group investigated the age-dependent changes of knee cartilage using a 3D MRF sequence for T_1, T_2, and $T_{1\rho}$ maps in healthy subjects.[89] Higher global and regional cartilage T_2 and $T_{1\rho}$ measurements were found for higher age groups as shown in Fig. 10.

A 3D MRF method was proposed for high-resolution (0.5 mm^2) knee cartilage PD, T_1, and T_2 mapping.[90] Different trajectories were implemented in the k_{xy} and k_z directions followed by the singular value decomposition (SVD) compression reconstruction method to reduce

reconstruction time. An algorithm was proposed to optimize the reconstruction of 3D MRF data.[91] The low-rank property of the data was exploited and a subspace projection scheme was adopted to improve the accuracy of parameter estimation. Significant improvements in MRF time-series images were observed based on numerical experiments, and the technique was able to provide more accurate parameter maps.

Machine learning models have been investigated with quantitative MRI maps derived from MRF cartilage data in recent years. The accuracy and feasibility of different machine learning models using quantitative MRI parameters in predicting cartilage matrix components were compared.[92] In this study, the ground truth was obtained from digital densitometry and polarized light microscopy. The Gaussian process regression (GPR) showed better performance than random forest, support vector regression, gradient boosting, and multilayer perceptron. A prospective, intraindividual ex vivo study was conducted to evaluate whether multiparametric quantitative MRI techniques could predict cartilage composition.[93] In the study, T_1, T_2, $T_{1\rho}$, and T_2^* parameter maps of the knee joints were used to train DL models with micro-spectroscopically determined local proteoglycan and collagen fibers contents as ground truth. The results showed that advanced machine learning techniques could be used to determine compositional features of cartilage based on quantitative parameters with potential implications for the diagnosis of early cartilage degeneration and the monitoring of therapeutic outcomes.

DL-Based Segmentation

Cartilage segmentation for morphometry is still one of the most challenging tasks for quantitative assessment of OA as described in a recent review.[48] Currently, DL approaches have been among the most commonly used and efficient methods for segmenting cartilage. Cartilage segmentation and quantification are important for understanding disease-related structural changes in subjects with or at risk for OA[46] and serve as a pre-requisite to extracting relevant cartilage compositional MRI biomarkers such as T_2 relaxation time.[94]

Manual segmentation, though usually used as a gold standard, is labor-intensive and subjective to operator bias and error. DL-based segmentation is a good alternative since it can be very fast. The recent development of DL methods for segmenting cartilage on knee MRI has been described in.[95–97] In the study,[95] a proposed 2D U-Net-based model showed high agreement with manual segmentation while preserving longitudinal reproducibility of quantitative cartilage morphometry from MRI knee datasets. In the study,[96] 3D convolutional neural networks (CNN) were used to investigate the 3D bone morphology in knee OA by segmenting the patella and distal femur cortex. The technique showed high accuracy in delineating the indistinct interfaces between bone and other joint structures. Transfer learning, also known as domain adaption, is a technique to transfer previously acquired knowledge to new problems (i.e. new datasets or tasks). In the study,[97] a GAN was combined with transfer learning using a small training dataset and showed comparable performance to humans in knee cartilage segmentation on heterogeneous knee MR images.

MRI-Based Biomechanical Assessment

Cartilage is a load-bearing structure and is subject to changes in biomechanical function with several factors including aging, trauma, pathology, and overuse. Recent techniques have shown the feasibility of compositional MRI in assessing cartilage overuse. The feasibility of T_2^* mapping of the knee cartilage in assessing the response to mechanical loading in skiing was demonstrated.[98] More specific biomechanical measures, such as strain mapping, were evaluated in the knee cartilage,[99] as shown in Fig. 11, and intervertebral discs.[100] Displacement encoding with stimulated echoes (DENSE) MRI was used on human cartilage during cyclic varus loading to assess displacement and strain.[101] Also in the study by,[101] $T_{1\rho}$ maps were acquired before and after varus loading to investigate changes with this kind of loading. This emerging topic shows the utility of assessing biomechanical function using noninvasive MRI methods under mechanical loading.

Summary of Discussion and Future Directions

Current Challenges of Emerging Methods

Although recent emerging quantitative MRI techniques have many advantages for accelerating cartilage compositional MRI, several challenges need to be addressed before their widespread application in musculoskeletal imaging. For example, the quality of many CS reconstructions depends on the choice of regularization parameters. In retrospective CS studies, the parameter is usually optimized to provide an image as similar as possible to the FS reference image. However, this is not possible in prospective studies leading to the need for methods for automatically choosing the regularization parameters.

Recently, DL methods showed promising initial results for image reconstruction, fully automated cartilage segmentation, and quantitative compositional mapping. One challenge when using DL approaches is the difficulty in obtaining large training datasets to optimize model performance. Simulated datasets have been recently used to generate large training datasets with good results. Alternatively, studies have utilized GANs to synthesize MR images for augmenting the training datasets. A more comprehensive investigation of the robustness and generalizability of DL-based cartilage compositional mapping techniques is also needed.

The MRF framework is highly flexible for multi-parametric cartilage mapping but still poses a significant computational burden and scan time as the dimensionality increases. Rigorous technical improvements and robust validations are necessary for pulse sequence optimization, faster image reconstructions, clinical pathology assessment, and quantitative metrics for error analysis before the widespread use of MRF for musculoskeletal imaging.

Standardization of Compositional MRI Techniques across Different Scanners, Vendors, and Institutions

T_2 and $T_{1\rho}$ mapping are by far the most common cartilage compositional MRI techniques used in clinical practice and OA research studies.[6] However, cartilage T_2 and $T_{1\rho}$ relaxation time are influenced by multiple factors including the type of scanner, coil, sequence, and imaging parameters used to obtain the measurement.[102,103] Coefficients of variation for

scan–rescan reproducibility for the six articular surfaces of the knee joint using the same scanner, coil, and imaging protocol have ranged between 2.3% and 6.5% for T_2 and between 4.2% and 7.4% for $T_{1\rho}$ with much higher coefficients of variance for sub-regional and laminar analysis.[104,105] This reproducibility is adequate for cross-sectional and longitudinal OA research studies performed at a single institution. However, additional standardization of cartilage T_2 and $T_{1\rho}$ measurements is needed for multicenter OA research studies and clinical trials.

Recent studies have investigated the scan–rescan reproducibility of cartilage compositional MRI techniques across different scanners, vendors, and institutions. Coefficients of variation for reproducibility of cartilage T_2 and $T_{1\rho}$ measurements of the knee joint for subjects evaluated at three separate institutions using the same 3 T scanner model from the same manufacturer with the same imaging protocols were 4.4% for T_2 and 4.9% for $T_{1\rho}$.[106] However, coefficients of variance increased to 10.1% for T_2 and 8.1% for $T_{1\rho}$ when the same imaging protocols were performed on three different 3 T scanner models from three different manufacturers.[107] Coefficients of variance were even higher when different compositional MRI sequences were used to measure cartilage T_2 and $T_{1\rho}$ on different scanner models from different manufacturers.[103,106,107] These inherent variations in cartilage T_2 and $T_{1\rho}$ relaxation time may serve as confounding factors that may make it challenging to detect changes in cartilage MRI biomarkers due to degeneration.

Current studies suggest that with careful quality control and cross-calibration, compositional MRI can be applied in multicenter research studies and clinical trials for evaluating cartilage degeneration if the same imaging protocol is used on the same scanner model from the same manufacturer.[106] However, additional future collaborative efforts between researchers and MRI vendors will be needed to accomplish the ultimate goal of better standardization of cartilage MRI biomarkers across different scanner models from different manufacturers at different institutions.[108] This will require all MRI vendors to agree on a single sequence for measuring cartilage T_2 and $T_{1\rho}$ relaxation time and then work together to limit variability in factors such as MRI system and coil design, B_0 homogeneity profiles, shimming algorithms, and reconstruction and postprocessing methods to better standardize quantitative measurements.[107]

Clinical Translational Impact on MSK Diseases

Quantitative MRI techniques are highly reliable for detecting early OA and assessing disease- and treatment-related changes in cartilage composition and ultrastructure.[6] However, the current widespread translation of cartilage compositional MRI techniques into clinical practice and multicenter research studies has been limited by multiple factors including long acquisition times, inefficient image analysis methods, and lack of standardization of quantitative MRI measurements. There have been many recent advances in compositional MRI pulse sequence acceleration which have greatly reduced acquisition times. New DL methods have also been described for rapid and fully automated cartilage segmentation, which is the first and most time-consuming step in the image analysis process. However, much additional work is needed to improve the standardization of cartilage compositional MRI techniques.

Standardization of rapidly acquired and efficiently analyzed cartilage MRI biomarkers would allow for large multicenter OA research studies and a better comparison of quantitative imaging data acquired at different institutions. Cartilage T_2 measurements obtained on older adults in the Osteoarthritis Initiative (OAI) have led to a wealth of important information on knee OA.[109] Imagine the potential knowledge obtained if rapidly acquired measurements of cartilage T_2 and $T_{1\rho}$ could be standardized and analyzed from larger and more diverse patient populations as part of routine clinical care at hundreds of institutions worldwide. Larger patient populations evaluated during a clinical knee MRI examination would facilitate cost-effective research for a better understanding of disease mechanisms and a more rapid evaluation of new surgical and pharmaceutical therapies. In addition, standardization of cartilage MRI biomarkers would allow for the development of normative data for cartilage T_2 and $T_{1\rho}$ relaxation times on different articular surfaces for individuals of different ages, gender, and ethnicity. The development of normative data and threshold values could be used to define abnormal cartilage compositional values and values associated with different disease burdens and different risks for disease onset and progression.

Summary

This review of compositional cartilage MRI has systematically introduced and discussed the current state-of-the-art methods as well as recent emerging techniques for the quantitative assessment of cartilage. The potential challenges and opportunities for emerging techniques were also discussed including standardization across different scanners, vendors, and institutions. It is expected that some of these emerging accelerated cartilage compositional MRI techniques will be translated to widespread clinical use in the near future to improve the detection of disease onset and progression, enhance treatment monitoring, and ultimately aid in the management of patient care.

Grant Support:

This study supported NIH grants R21 AR075259, R21 AR078357, R01 AR068966, R01 AR076328, R01 AR076985, and R01-AR078308–01A1, performed under the Center of Advanced Imaging Innovation and Research (CAI2R) at NYU Grossman School of Medicine and NIBIB Biomedical Technology Resource Center (NIH P41 EB017183).

References

1. Bliddal H, Leeds AR, Christensen R. Osteoarthritis, obesity and weight loss: Evidence, hypotheses and horizons – A scoping review. Obes Rev 2014;15:578–586. 10.1111/obr.12173. [PubMed: 24751192]
2. Helmick CG, Felson DT, Lawrence RC, et al. Estimates of the prevalence of arthritis and other rheumatic conditions in the United States: Part I. Arthritis Rheum 2008;58:15–25. 10.1002/art.23177. [PubMed: 18163481]
3. Crema MD, Nevitt MC, Guermazi A, et al. Progression of cartilage damage and meniscal pathology over 30 months is associated with an increase in radiographic tibiofemoral joint space narrowing in persons with knee OA – The MOST study. Osteoarthr Cartil 2014;22:1743–1747. 10.1016/j.joca.2014.07.008.
4. Sophia Fox AJ, Bedi A, Rodeo SA. The basic science of articular cartilage: Structure, composition, and function. Sports Health 2009;1:461–468. 10.1177/1941738109350438. [PubMed: 23015907]

5. Maroudas A, Bayliss MT, Venn MF. Further studies on the composition of human femoral head cartilage. Ann Rheum Dis 1980;39:514–523. 10.1136/ard.39.5.514. [PubMed: 7436585]
6. Guermazi A, Alizai H, Crema MD, Trattnig S, Regatte RR, Roemer FW. Compositional MRI techniques for evaluation of cartilage degeneration in osteoarthritis. Osteoarthr Cartil 2015;23:1639–1653. 10.1016/j.joca.2015.05.026.
7. Friedrich KM, Shepard T, de Oliveira VS, et al. T2 measurements of cartilage in osteoarthritis patients with meniscal tears. Am J Roentgenol 2009;193:W411–W415. 10.2214/AJR.08.2256. [PubMed: 19843720]
8. Marik W, Apprich S, Welsch GH, Mamisch TC, Trattnig S. Biochemical evaluation of articular cartilage in patients with osteochondrosis dissecans by means of quantitative T2- and T2*-mapping at 3T MRI: A feasibility study. Eur J Radiol 2012;81:923–927. 10.1016/j.ejrad.2011.01.124. [PubMed: 21392912]
9. Golditz T, Steib S, Pfeifer K, et al. Functional ankle instability as a risk factor for osteoarthritis: Using T2-mapping to analyze early cartilage degeneration in the ankle joint of young athletes. Osteoarthr Cartil 2014;22:1377–1385. 10.1016/j.joca.2014.04.029.
10. Xia Y, Moody JB, Alhadlaq H. Orientational dependence of T2 relaxation in articular cartilage: A microscopic MRI (uMRI) study. Magn Reson Med 2002;48:460–469. 10.1002/mrm.10216. [PubMed: 12210910]
11. Nishioka H, Hirose J, Nakamura E, et al. T1ρ and T2 mapping reveal the in vivo extracellular matrix of articular cartilage. J Magn Reson Imaging 2012;35:147–155. 10.1002/jmri.22811. [PubMed: 21990043]
12. Binks DA, Hodgson RJ, Ries ME, et al. Quantitative parametric MRI of articular cartilage: A review of progress and open challenges. Br J Radiol 2013;86:20120163. 10.1259/bjr.20120163. [PubMed: 23407427]
13. Staroswiecki E, Granlund KL, Alley MT, Gold GE, Hargreaves BA. Simultaneous estimation of T2 and apparent diffusion coefficient in human articular cartilage in vivo with a modified three-dimensional double echo steady state (DESS) sequence at 3 T. Magn Reson Med 2012;67:1086–1096. 10.1002/mrm.23090. [PubMed: 22179942]
14. Hesper T, Hosalkar HS, Bittersohl D, et al. T2* mapping for articular cartilage assessment: Principles, current applications, and future prospects. Skeletal Radiol 2014;43:1429–1445. 10.1007/s00256-014-1852-3. [PubMed: 24643762]
15. Mars M, Tbini Z, Gharbi S, Bouaziz MC, Ladeb F. T2 versus T2* MRI mapping in the knee articular cartilage at 1.5 tesla and 3 tesla. Open Med J 2018;5:119–129. 10.2174/1874220301805010119.
16. Qian Y, Williams AA, Chu CR, Boada FE. Multicomponent T2* mapping of knee cartilage: Technical feasibility ex vivo. Magn Reson Med 2010;64:1426–1431. 10.1002/mrm.22450. [PubMed: 20865752]
17. Bittersohl B, Miese FR, Hosalkar HS, et al. T2* mapping of hip joint cartilage in various histological grades of degeneration. Osteoarthr Cartil 2012;20:653–660. 10.1016/j.joca.2012.03.011.
18. Du J, Takahashi AM, Chung CB. Ultrashort TE spectroscopic imaging (UTESI): Application to the imaging of short T2 relaxation tissues in the musculoskeletal system. J Magn Reson Imaging 2009;29:412–421. 10.1002/jmri.21465. [PubMed: 19161197]
19. Regatte RR, Akella SVS, Lonner JH, Kneeland JB, Reddy R. T1ρ relaxation mapping in human osteoarthritis (OA) cartilage: Comparison of T1ρ with T2. J Magn Reson Imaging 2006;23:547–553. 10.1002/jmri.20536. [PubMed: 16523468]
20. Akella SVS, Reddy Regatte R, Gougoutas AJ, et al. Proteoglycan-induced changes in T1ρ-relaxation of articular cartilage at 4T. Magn Reson Med 2001;46:419–423. 10.1002/mrm.1208. [PubMed: 11550230]
21. Duvvuri U, Goldberg AD, Kranz JK, et al. Water magnetic relaxation dispersion in biological systems: The contribution of proton exchange and implications for the noninvasive detection of cartilage degradation. Proc Natl Acad Sci 2001;98:12479–12484. 10.1073/pnas.221471898. [PubMed: 11606754]

22. Wheaton AJ, Casey FL, Gougoutas AJ, et al. Correlation of T1rho with fixed charge density in cartilage. J Magn Reson Imaging 2004;20:519–525. 10.1002/jmri.20148. [PubMed: 15332262]
23. Duvvuri U, Kudchodkar S, Reddy R, Leigh JS. T1ρ relaxation can assess longitudinal proteoglycan loss from articular cartilage in vitro. Osteoarthr Cartil 2002;10:838–844. 10.1053/joca.2002.0826.
24. Li X, Cheng J, Lin K, et al. Quantitative MRI using T1ρ and T2 in human osteoarthritic cartilage specimens: Correlation with biochemical measurements and histology. Magn Reson Imaging 2011;29:324–334. 10.1016/j.mri.2010.09.004. [PubMed: 21130590]
25. Keenan KE, Besier TF, Pauly JM, et al. Prediction of glycosaminoglycan content in human cartilage by age, T1ρ and T2 MRI. Osteoarthr Cartil 2011;19:171–179. 10.1016/j.joca.2010.11.009.
26. Stahl R, Luke A, Li X, et al. T1rho, T2 and focal knee cartilage abnormalities in physically active and sedentary healthy subjects versus early OA patients—A 3.0-tesla MRI study. Eur Radiol 2009;19:132–143. 10.1007/s00330-008-1107-6. [PubMed: 18709373]
27. Bashir A, Gray ML, Hartke J, Burstein D. Nondestructive imaging of human cartilage glycosaminoglycan concentration by MRI. Magn Reson Med 1999;41:857–865. 10.1002/(SICI)1522-2594(199905)41:5<857::AID-MRM1>3.0.CO;2-E. [PubMed: 10332865]
28. Nieminen MT, Rieppo J, Silvennoinen J, et al. Spatial assessment of articular cartilage proteoglycans with Gd-DTPA-enhanced T1 imaging. Magn Reson Med 2002;48:640–648. 10.1002/mrm.10273. [PubMed: 12353281]
29. Kurkijärvi JE, Nissi MJ, Kiviranta I, Jurvelin JS, Nieminen MT. Delayed gadolinium-enhanced MRI of cartilage (dGEMRIC) and T 2 characteristics of human knee articular cartilage: Topographical variation and relationships to mechanical properties. Magn Reson Med 2004;52:41–46. 10.1002/mrm.20104. [PubMed: 15236365]
30. Tiderius CJ, Olsson LE, Leander P, Ekberg O, Dahlberg L. Delayed gadolinium-enhanced MRI of cartilage (dGEMRIC) in early knee osteoarthritis. Magn Reson Med 2003;49:488–492. 10.1002/mrm.10389. [PubMed: 12594751]
31. Robson MD, Gatehouse PD, Bydder M, Bydder GM. Magnetic resonance: An Introduction to ultrashort TE (UTE) imaging. J Comput Assist Tomogr 2003;27:825–846. 10.1097/00004728-200311000-00001. [PubMed: 14600447]
32. Grodzki DM, Jakob PM, Heismann B. Ultrashort echo time imaging using pointwise encoding time reduction with radial acquisition (PETRA). Magn Reson Med 2012;67:510–518. 10.1002/mrm.23017. [PubMed: 21721039]
33. Ling W, Regatte RR, Navon G, Jerschow A. Assessment of glycosaminoglycan concentration in vivo by chemical exchange-dependent saturation transfer (gagCEST). Proc Natl Acad Sci 2008;105:2266–2270. 10.1073/pnas.0707666105. [PubMed: 18268341]
34. Rehnitz C, Kupfer J, Streich NA, et al. Comparison of biochemical cartilage imaging techniques at 3 T MRI. Osteoarthr Cartil 2014;22:1732–1742. 10.1016/j.joca.2014.04.020.
35. Wheaton AJ, Borthakur A, Shapiro EM, et al. Proteoglycan loss in human knee cartilage: Quantitation with sodium MR imaging—Feasibility study. Radiology 2004;231:900–905. 10.1148/radiol.2313030521. [PubMed: 15163825]
36. Madelin G, Babb J, Xia D, et al. Articular cartilage: Evaluation with fluid-suppressed 7.0-T sodium MR imaging in subjects with and subjects without osteoarthritis. Radiology 2013;268:481–491. 10.1148/radiol.13121511. [PubMed: 23468572]
37. Trattnig S, Welsch GH, Juras V, et al. 23Na MR imaging at 7 T after knee matrix-associated autologous chondrocyte transplantation: Preliminary results. Radiology 2010;257:175–184. 10.1148/radiol.10100279. [PubMed: 20713608]
38. Brown R, Madelin G, Lattanzi R, et al. Design of a nested eight-channel sodium and four-channel proton coil for 7T knee imaging. Magn Reson Med 2013;70:259–268. 10.1002/mrm.24432. [PubMed: 22887123]
39. Raya JG, Melkus G, Adam-Neumair S, et al. Change of diffusion tensor imaging parameters in articular cartilage with progressive proteoglycan extraction. Invest Radiol 2011;46:401–409. 10.1097/RLI.0b013e3182145aa8. [PubMed: 21427593]

40. Deng X, Farley M, Nieminen MT, Gray M, Burstein D. Diffusion tensor imaging of native and degenerated human articular cartilage. Magn Reson Imaging 2007;25:168–171. 10.1016/j.mri.2006.10.015. [PubMed: 17275610]
41. Raya JG, Arnoldi AP, Weber DL, et al. Ultra-high field diffusion tensor imaging of articular cartilage correlated with histology and scanning electron microscopy. Magn Reson Mater Physics, Biol Med 2011;24: 247–258. 10.1007/s10334-011-0259-6.
42. Raya JG, Melkus G, Adam-Neumair S, et al. Diffusion-tensor imaging of human articular cartilage specimens with early signs of cartilage damage. Radiology 2013;266:831–841. 10.1148/radiol.12120954. [PubMed: 23238155]
43. Raya JG, Horng A, Dietrich O, et al. Articular cartilage: In vivo diffusion-tensor imaging. Radiology 2012;262:550–559. 10.1148/radiol.11110821. [PubMed: 22106350]
44. Deoni SCL, Peters TM, Rutt BK. Quantitative diffusion imaging with steady-state free precession. Magn Reson Med 2004;51:428–433. 10.1002/mrm.10708. [PubMed: 14755673]
45. Bieri O, Ganter C, Scheffler K. Quantitative in vivo diffusion imaging of cartilage using double echo steady-state free precession. Magn Reson Med 2012;68:720–729. 10.1002/mrm.23275. [PubMed: 22161749]
46. Wirth W, Ladel C, Maschek S, Wisser A, Eckstein F, Roemer F. Quantitative measurement of cartilage morphology in osteoarthritis: Current knowledge and future directions. Skeletal Radiol 2022. 10.1007/s00256-022-04228-w.
47. Dam EB, Desai AD, Deniz CM, et al. Towards automatic cartilage quantification in clinical trials – Continuing from the 2019 IWOAI Knee Segmentation Challenge. Osteoarthr Imaging 2023;100087. 10.1016/j.ostima.2023.100087.
48. Chaudhari AS, Kogan F, Pedoia V, Majumdar S, Gold GE, Hargreaves BA. Rapid knee MRI acquisition and analysis techniques for imaging osteoarthritis. J Magn Reson Imaging 2020;52:1321–1339. 10.1002/jmri.26991. [PubMed: 31755191]
49. Feng L, Ma D, Liu F. Rapid MR relaxometry using deep learning: An overview of current techniques and emerging trends. NMR Biomed 2022;35:e4416. 10.1002/nbm.4416. [PubMed: 33063400]
50. Lin DJ, Walter SS, Fritz J. Artificial intelligence–Driven ultra-fast super-resolution MRI. Invest Radiol 2023;58:28–42. 10.1097/RLI.0000000000000928. [PubMed: 36355637]
51. Liu Y, Ying L, Chen W, et al. Accelerating the 3D T1ρ mapping of cartilage using a signal-compensated robust tensor principal component analysis model. Quant Imaging Med Surg 2021;11:3376–3391. 10.21037/qims-20-790. [PubMed: 34341716]
52. Hüfken T, Arbogast JM, Bracher A-K, Beer M, Neubauer H, Rasche V. Accelerated model-based quantitative diffusion MRI: A feasibility study for musculoskeletal application. Z Med Phys 2022;32:240–247. 10.1016/j.zemedi.2021.04.004. [PubMed: 34175164]
53. Wahid A, Shah JA, Khan AU, Ahmed M, Razali H. Multi-layer basis pursuit for compressed sensing MR image reconstruction. IEEE Access 2020;8:186222–186232. 10.1109/ACCESS.2020.3028877.
54. Zibetti MVW, Johnson PM, Sharafi A, Hammernik K, Knoll F, Regatte RR. Rapid mono and biexponential 3D-T1ρ mapping of knee cartilage using variational networks. Sci Rep 2020;10:19144. 10.1038/s41598-020-76126-x. [PubMed: 33154515]
55. Radmanesh A, Muckley MJ, Murrell T, et al. Exploring the acceleration limits of deep learning variational network-based two-dimensional brain MRI. Radiol Artif Intell 2022;4:4. 10.1148/ryai.210313.
56. Kim M, Lee S-M, Park C, et al. Deep learning-enhanced parallel imaging and simultaneous multislice acceleration reconstruction in knee MRI. Invest Radiol 2022;57:826–833. 10.1097/RLI.0000000000000900. [PubMed: 35776434]
57. Calivà F, Namiri NK, Dubreuil M, Pedoia V, Ozhinsky E, Majumdar S. Studying osteoarthritis with artificial intelligence applied to magnetic resonance imaging. Nat Rev Rheumatol 2022;18:112–121. 10.1038/s41584-021-00719-7. [PubMed: 34848883]
58. Li Y, Li J, Ma F, Du S, Liu Y. High quality and fast compressed sensing MRI reconstruction via edge-enhanced dual discriminator generative adversarial network. Magn Reson Imaging 2021;77:124–136. 10.1016/j.mri.2020.12.011. [PubMed: 33359427]

59. Tolpadi AA, Han M, Calivà F, Pedoia V, Majumdar S. Region of interest-specific loss functions improve T2 Quantification with ultrafast T2 mapping MRI sequences in knee, hip and lumbar spine. Sci Rep 2023;12(1):22208.
60. Chaudhari AS, Grissom MJ, Fang Z, et al. Diagnostic accuracy of quantitative multicontrast 5-minute knee MRI using prospective artificial intelligence image quality enhancement. Am J Roentgenol 2021; 216:1614–1625. 10.2214/AJR.20.24172. [PubMed: 32755384]
61. Desai AD, Schmidt AM, Rubin EB, et al. SKM-TEA: A dataset for accelerated MRI reconstruction with dense image labels for quantitative clinical evaluation. arXiv Prepr 2022;1–22. https://arxiv.org/abs/2203.06823.
62. Desai AD, Gunel B, Ozturkler BM, et al. VORTEX: Physics-driven data augmentations using consistency training for robust accelerated MRI reconstruction. arXiv Prepr 2021;1–26. https://arxiv.org/abs/2111.02549.
63. Desai AD, Ozturkler BM, Sandino CM, et al. Noise2Recon: enabling joint MRI reconstruction and denoising with semi-supervised and self-supervised learning. arXiv Prepr 2021.
64. Zibetti MVW, Knoll F, Regatte RR. Alternating learning approach for variational networks and undersampling pattern in parallel MRI applications. IEEE Trans Comput Imaging 2022;8:449–461. 10.1109/TCI.2022.3176129. [PubMed: 35795003]
65. Li H, Yang M, Kim JH, et al. SuperMAP: Deep ultrafast MR relaxometry with joint spatiotemporal undersampling. Magn Reson Med 2023;89(1):64–76. 10.1002/mrm.29411. [PubMed: 36128884]
66. Liu S, Li H, Liu Y, et al. Highly accelerated MR parametric mapping by undersampling the k-space and reducing the contrast number simultaneously with deep learning. Phys Med Biol 2022;67(18): 185004. 10.1088/1361-6560/ac8c81.
67. Liu F, Kijowski R, Feng L, El Fakhri G. High-performance rapid MR parameter mapping using model-based deep adversarial learning. Magn Reson Imaging 2020;74:152–160. 10.1016/j.mri.2020.09.021. [PubMed: 32980503]
68. Liu F, Kijowski R, El Fakhri G, Feng L. Magnetic resonance parameter mapping using model-guided self-supervised deep learning. Magn Reson Med 2021;85:3211–3226. 10.1002/mrm.28659. [PubMed: 33464652]
69. Zibetti MVW, Sharafi A, Regatte RR. Optimization of spin-lock times in T1ρ mapping of knee cartilage: Cramér-Rao bounds versus matched sampling-fitting. Magn Reson Med 2022;87:1418–1434. 10.1002/mrm.29063. [PubMed: 34738252]
70. de Moura HL, Menon RG, Zibetti MVW, Regatte RR. Optimization of spin-lock times for T1ρ mapping of human knee cartilage with bi- and stretched-exponential models. Sci Rep 2022;12:16829. 10.1038/s41598-022-21269-2. [PubMed: 36207361]
71. Peng Q, Wu C, Kim J, Li X. Efficient phase-cycling strategy for high-resolution 3D gradient-echo quantitative parameter mapping. NMR Biomed 2022;35(7):e4700. 10.1002/nbm.4700. [PubMed: 35068007]
72. Han M, Tibrewala R, Bahroos E, Pedoia V, Majumdar S. Magnetization-prepared spoiled gradient-echo snapshot imaging for efficient measurement of R 2-R 1ρ in knee cartilage. Magn Reson Med 2022; 87:733–745. 10.1002/mrm.29024. [PubMed: 34590728]
73. Zibetti MVW, De Moura HL, Keerthivasan MB, Regatte RR. Optimizing variable flip-angles in magnetization-prepared gradient echo sequences for efficient 3D-T1rho mapping. arXiv Prepr 2022;1–27. https://arxiv.org/abs/2211.09214.
74. Yang Y, Chen Z, Xu X, Liu Y, Zhu Y, Liang D. The optimization of adiabatic pulses with constant amplitude spin-lock for magnetic resonance T1rho imaging 2021 IEEE international conference on real-time computing and robotics (RCAR), Vol 790: IEEE, Xining, China; 2021. p 1170–1175. 10.1109/RCAR52367.2021.9517352.
75. Pang Y A self-compensated spin-locking scheme for quantitative R1rho dispersion MR imaging in ordered tissues. Magn Reson Imaging 2022;94:112–118. 10.1016/j.mri.2022.09.007. [PubMed: 36181969]
76. Gram M, Seethaler M, Jakob PM, Nordbeck P. Balanced spin-lock preparation for B1-insensitive and B0-insensitive quantification of the rotating frame relaxation time T1ρ. Magn Reason Med 2021;85(5): 2771–2780. 10.1002/mrm.28585.

77. Zijlstra F, Seevinck PR. Multiple-echo steady-state (MESS): Extending DESS for joint T 2 mapping and chemical-shift corrected water-fat separation. Magn Reson Med 2021;86:3156–3165. 10.1002/mrm.28921. [PubMed: 34270127]

78. Barbieri M, Chaudhari AS, Moran CJ, Gold GE, Hargreaves BA, Kogan F. A method for measuring B 0 field inhomogeneity using quantitative double-echo in steady-state. Magn Reson Med 2023;89: 577–593. 10.1002/mrm.29465. [PubMed: 36161727]

79. Afsahi AM, Sedaghat S, Moazamian D, et al. Articular cartilage assessment using ultrashort echo time MRI: A review. Front Endocrinol (Lausanne) 2022;13:1–17. 10.3389/fendo.2022.892961.

80. Cheng KY, Moazamian D, Ma Y, et al. Clinical application of ultrashort echo time (UTE) and zero echo time (ZTE) magnetic resonance (MR) imaging in the evaluation of osteoarthritis. Skeletal Radiol 2023. 10.1007/s00256-022-04269-1.

81. Wu M, Ma Y-J, Liu M, et al. Quantitative assessment of articular cartilage degeneration using 3D ultrashort echo time cones adiabatic T1ρ (3D UTE-cones-AdiabT1ρ) imaging. Eur Radiol 2022;32:6178–6186. 10.1007/s00330-022-08722-6. [PubMed: 35357540]

82. Wu M, Ma Y, Kasibhatla A, et al. Convincing evidence for magic angle less-sensitive quantitative T 1ρ imaging of articular cartilage using the 3D ultrashort echo time cones adiabatic T 1ρ (3D UTE cones-AdiabT 1ρ) sequence. Magn Reson Med 2020;84:2551–2560. 10.1002/mrm.28317. [PubMed: 32419199]

83. Wilson R, Bowen L, Kim W, Reiter D, Neu C. Stretched-exponential modeling of anomalous T1ρ and T2 relaxation in the intervertebral disc In vivo. bioRxiv 2020;2020.05.21.109785. 10.1101/2020.05.21.109785.

84. Jang H, McMillan AB, Ma Y, et al. Rapid single scan ramped hybrid-encoding for bicomponent T2* mapping in a human knee joint: A feasibility study. NMR Biomed 2020;33:1–10. 10.1002/nbm.4391.

85. Lu X, Jerban S, Wan L, et al. Three-dimensional ultrashort echo time imaging with tricomponent analysis for human cortical bone. Magn Reson Med 2019;82:348–355. 10.1002/mrm.27718. [PubMed: 30847989]

86. Ma D, Gulani V, Seiberlich N, et al. Magnetic resonance fingerprinting. Nature 2013;495:187–192. 10.1038/nature11971. [PubMed: 23486058]

87. Sharafi A, Zibetti MVW, Chang G, Cloos M, Regatte RR. MR fingerprinting for rapid simultaneous T1, T2, and T1ρ relaxation mapping of the human articular cartilage at 3T. Magn Reson Med 2020;84:2636–2644. 10.1002/mrm.28308. [PubMed: 32385949]

88. Sharafi A, Zibetti MVW, Chang G, Cloos MA, Regatte RR. Simultaneous bilateral T(1), T(2), and T(1ρ) relaxation mapping of the hip joint with magnetic resonance fingerprinting. NMR Biomed 2022;35:35. 10.1002/nbm.4651.

89. Kijowski R, Sharafi A, Zibetti MVW, Chang G, Cloos MA, Regatte RR. Age-dependent changes in knee cartilage T1, T2, and T1p simultaneously measured using MRI fingerprinting. J Magn Reson Imaging 2022. 10.1002/jmri.28451.

90. Han D, Hong T, Lee Y, Kim D-H. High resolution 3D magnetic resonance fingerprinting with hybrid radial-interleaved EPI acquisition for knee cartilage T1, T2 mapping. Investig Magn Reson Imaging 2021; 25:141. 10.13104/imri.2021.25.3.141.

91. Hu Y, Li P, Chen H, Zou L, Wang H. High-quality MR fingerprinting reconstruction using structured Low-rank matrix completion and sub-space projection. IEEE Trans Med Imaging 2022;41:1150–1164. 10.1109/TMI.2021.3133329. [PubMed: 34871169]

92. Mirmojarabian SA, Kajabi AW, Ketola JHJ, et al. Machine learning prediction of collagen fiber orientation and proteoglycan content from multiparametric quantitative MRI in articular cartilage. J Magn Reson Imaging 2023;57(4):1056–1068. 10.1002/jmri.28353. [PubMed: 35861162]

93. Linka K, Thüring J, Rieppo L, et al. Machine learning-augmented and microspectroscopy-informed multiparametric MRI for the non-invasive prediction of articular cartilage composition. Osteoarthr Cartil 2021; 29:592–602. 10.1016/j.joca.2020.12.022.

94. Pedoia V, Lee J, Norman B, Link TM, Majumdar S. Diagnosing osteoarthritis from T2 maps using deep learning: An analysis of the entire osteoarthritis initiative baseline cohort. Osteoarthr Cartil 2019;27: 1002–1010. 10.1016/j.joca.2019.02.800.

95. Wirth W, Eckstein F, Kemnitz J, et al. Accuracy and longitudinal reproducibility of quantitative femorotibial cartilage measures derived from automated U-net-based segmentation of two different MRI contrasts: Data from the osteoarthritis initiative healthy reference cohort. Magn. Reson. Mater. Physics, Biol. Med 2021;34:337–354. 10.1007/s10334-020-00889-7.

96. Cheng R, Alexandridi NA, Smith RM, et al. Fully automated patellofemoral MRI segmentation using holistically nested networks: Implications for evaluating patellofemoral osteoarthritis, pain, injury, pathology, and adolescent development. Magn Reson Med 2020;83: 139–153. 10.1002/mrm.27920. [PubMed: 31402520]

97. Yang M, Colak C, Chundru KK, et al. Automated knee cartilage segmentation for heterogeneous clinical MRI using generative adversarial networks with transfer learning. Quant Imaging Med Surg 2022;12: 2620–2633. 10.21037/qims-21-459. [PubMed: 35502381]

98. Schütz U, Martensen T, Kleiner S, et al. T2*-mapping of knee cartilage in response to mechanical loading in alpine skiing: A feasibility study. Diagnostics 2022;12:1391. 10.3390/diagnostics12061391. [PubMed: 35741201]

99. Menon RG, Zibetti MVW, Regatte RR. In vivo tibiofemoral cartilage strain mapping under static mechanical loading using continuous GRASP-MRI. J Magn Reson Imaging 2020;51:51–434. 10.1002/jmri.26859.

100. Menon RG, Zibetti MVW, Pendola M, Regatte RR. Measurement of three-dimensional internal dynamic strains in the intervertebral disc of the lumbar spine with mechafaonical loading and Golden-angle radial sparse parallel-magnetic resonance imaging. J Magn Reson Imaging 2021;54(2):486–496. 10.1002/jmri.27591. [PubMed: 33713520]

101. Lee W, Miller EY, Zhu H, Schneider SE, Reiter DA, Neu CP. Multiframe biomechanical and relaxometry analysis during in vivo loading of the human knee by spiral dualMRI and compressed sensing. bioRxiv 2023;1–27. 10.1101/2023.02.12.528211.

102. Pai A, Li X, Majumdar S. A comparative study at 3 T of sequence dependence of T2 quantitation in the knee. Magn Reson Imaging 2008;26:1215–1220. 10.1016/j.mri.2008.02.017. [PubMed: 18502073]

103. Balamoody S, Williams TG, Wolstenholme C, et al. Magnetic resonance transverse relaxation time T2 of knee cartilage in osteoarthritis at 3-T: A cross-sectional multicentre, multivendor reproducibility study. Skeletal Radiol 2013;42:511–520. 10.1007/s00256-012-1511-5. [PubMed: 23053200]

104. MacKay JW, Low SBL, TO S, Toms AP, McCaskie AW, Gilbert FJ. Systematic review and meta-analysis of the reliability and discriminative validity of cartilage compositional MRI in knee osteoarthritis. Osteoarthr Cartil 2018;26:1140–1152. 10.1016/j.joca.2017.11.018.

105. Atkinson HF, Birmingham TB, Moyer RF, et al. MRI T2 and T1ρ relaxation in patients at risk for knee osteoarthritis: A systematic review and meta-analysis. BMC Musculoskelet Disord 2019;20:1–18. 10.1186/s12891-019-2547-7. [PubMed: 30611236]

106. Li X, Pedoia V, Kumar D, et al. Cartilage T1ρ and T2 relaxation times: Longitudinal reproducibility and variations using different coils MR systems and sites. Osteoarthr Cartil 2015;23:2214–2223. 10.1016/j.joca.2015.07.006.

107. Kim J, Mamoto K, Lartey R, et al. Multi-vendor multi-site T1ρ and T2 quantification of knee cartilage. Osteoarthr Cartil 2020;28:1539–1550. 10.1016/j.joca.2020.07.005.

108. Chalian M, Li X, Guermazi A, et al. The QIBA profile for MRI-based compositional imaging of knee cartilage. Radiology 2021;301:423–432. 10.1148/radiol.2021204587. [PubMed: 34491127]

109. Eckstein F, Kwoh CK, Link TM. Imaging research results from the osteoarthritis initiative (OAI): A review and lessons learned 10 years after start of enrolment. Ann Rheum Dis 2014;73:1289–1300. 10.1136/annrheumdis-2014-205310. [PubMed: 24728332]

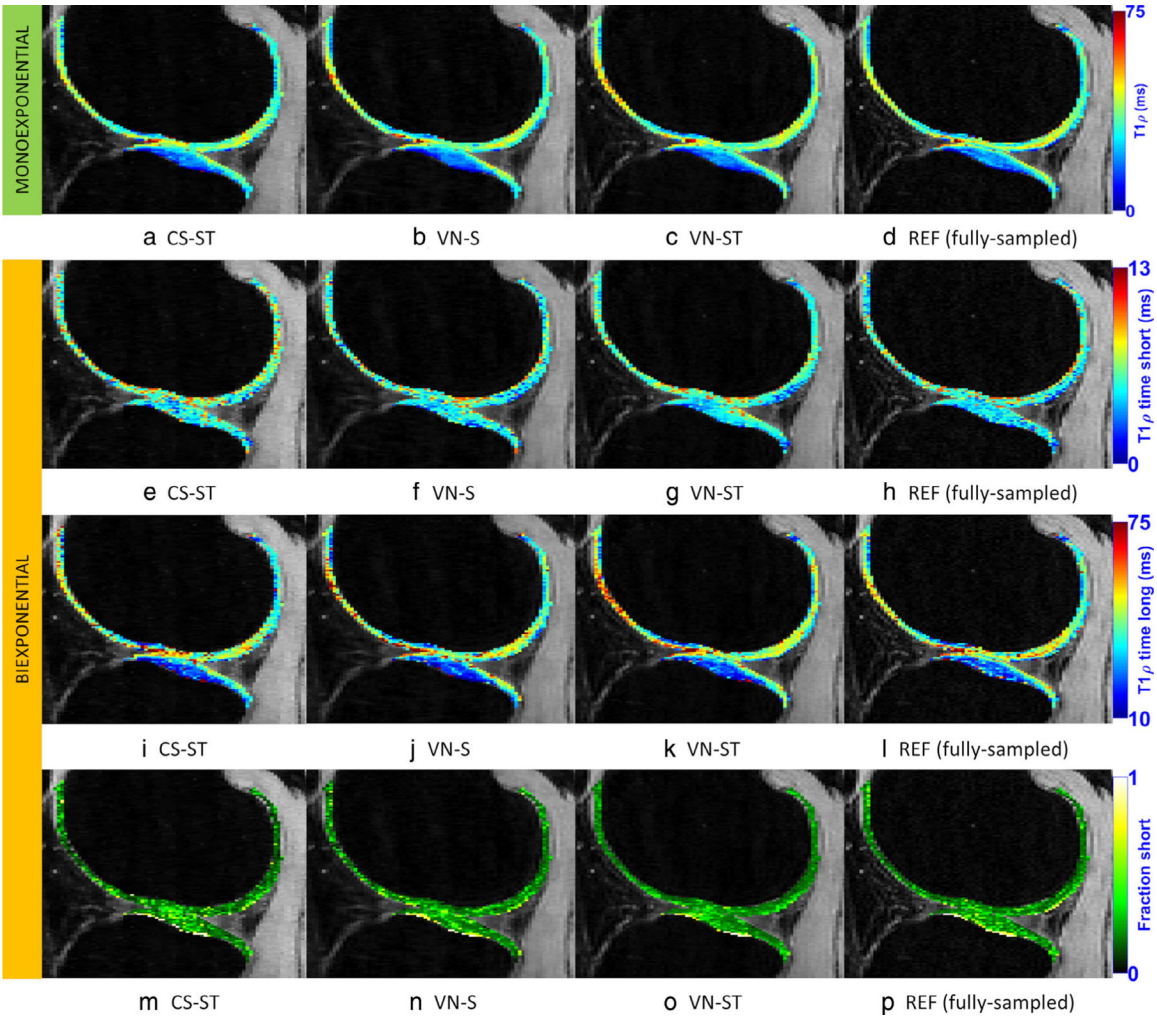

FIGURE 1:

Zibetti et al[54] compared compressed sensing (CS) with a spatiotemporal finite difference (CS-ST) against variational networks (VN) using independent spatial reconstructions (VN-S) and joint spatiotemporal reconstructions (VN-ST) with an acceleration factor of $R = 6$ on mono- and bi-exponential $T_{1\rho}$ relaxation models.

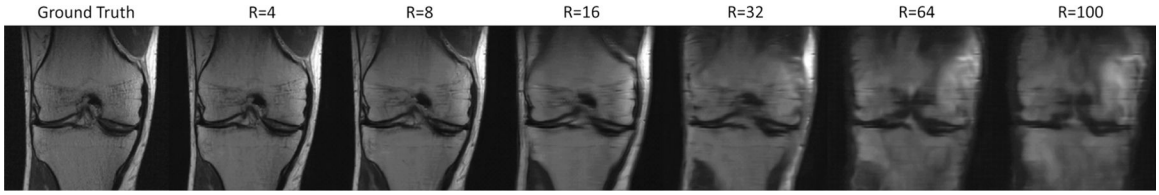

FIGURE 2:
Radmanesh et al[55] explored the limits of acceleration using a network based on the variational network (VN) for 2D acquisitions. *Source*: Images courtesy of Dr. Matthew Muckley, PhD, Meta AI, USA.

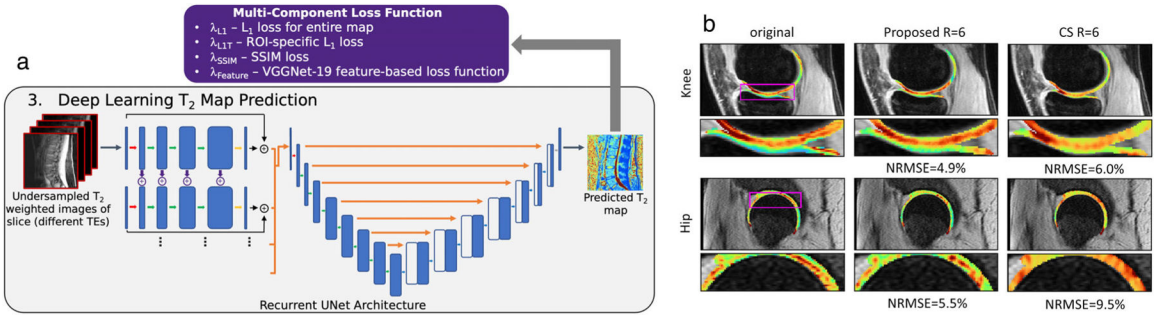

FIGURE 3:

The loss function used for deep-learning (DL) training contains a specific region of interest loss.[59] The neural network was trained to improve the accelerated MRI specifically in cartilage regions. *Source*: Images courtesy of Mr. Aniket Topaldi, University of California at San Francisco, USA.

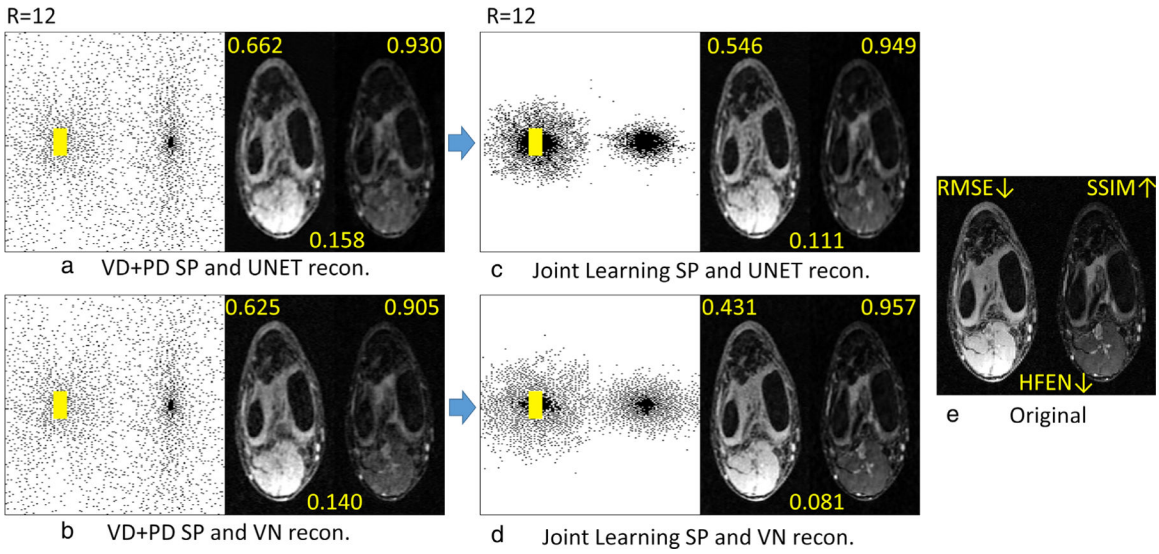

FIGURE 4:

Joint learning of the sampling pattern (SP) and deep-learning (DL) reconstruction was proposed, showing improvements over only learning of a DL reconstruction and a fixed SP.[64] Note that the variable density with Poisson disc (VD + PD) SP is one of the best human-made SPs for accelerated MRI. (a) VD + PD SP and UNET recon. (b) VD + PD SP and VN recon. (c) Joint learning SP and UNET recon. (d) Joint learning SP and VN recon.

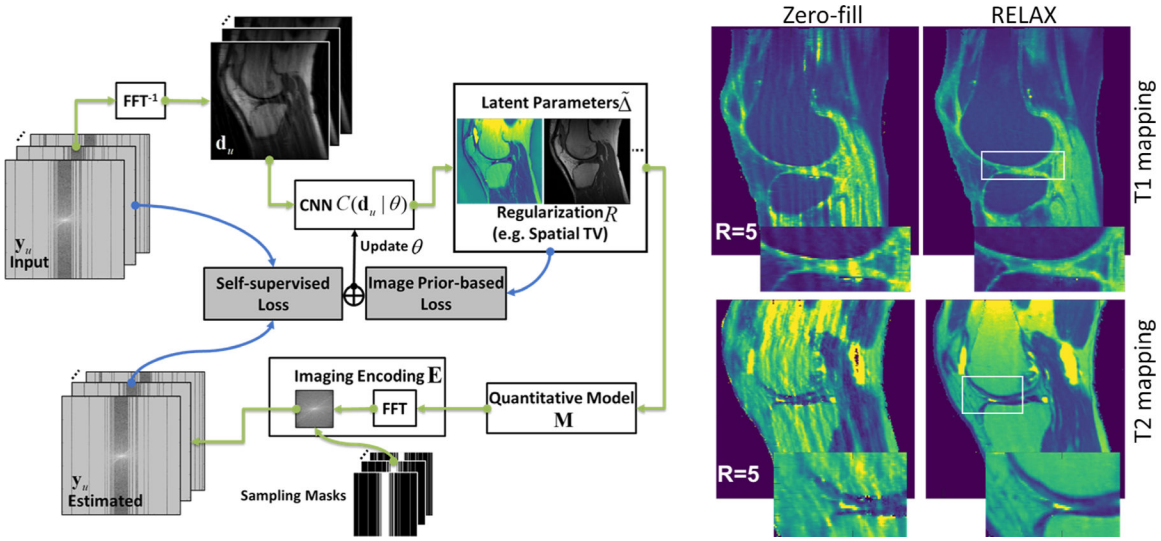

FIGURE 5:

Self-supervised learning for quantitative mapping with neural networks was proposed, where no reference images were needed for the learning process.[67] The method relays on k-space consistency and image priors. *Source*: Images courtesy of Dr. Fang Liu, PhD, Harvard Medical School, USA.

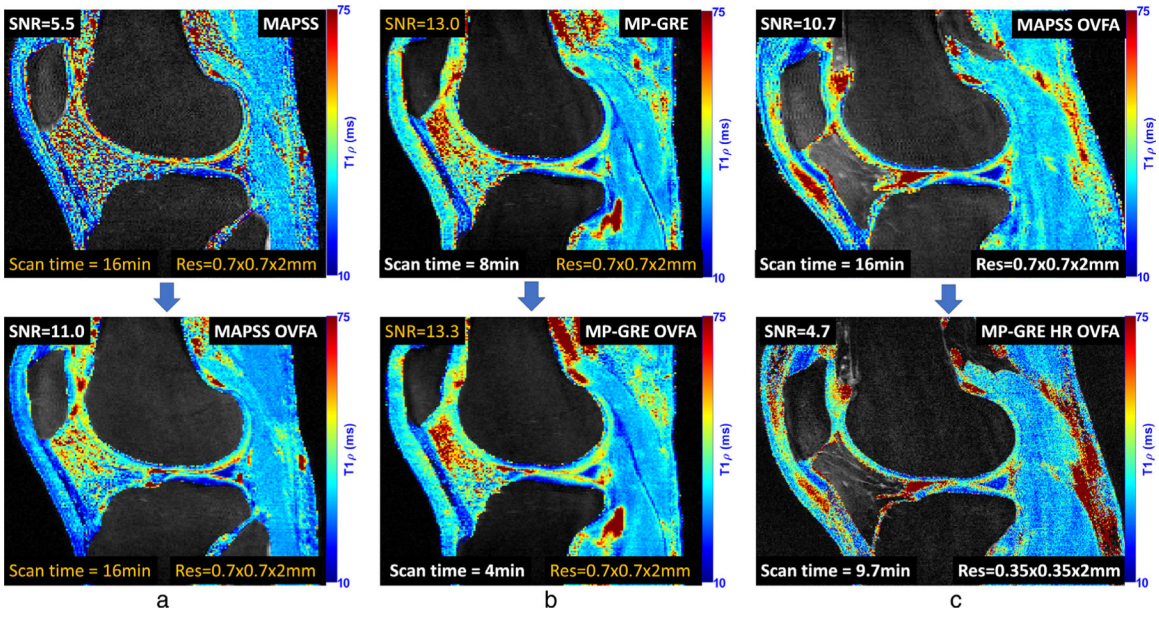

FIGURE 6:

Examples of the use of data-driven optimal variable flip-angles (OVFA) in $T_{1\rho}$ mapping.[73] The OVFA methods can be used to improve the SNR of magnetization-prepared angle-modulated partitioned k-space spoiled gradient echo snapshots (MAPSS), as in (a); to reduce the scan time of magnetization-prepared spoiled gradient echo (MP-GRE), as in (b); or even for other objectives, such as better resolution with less scan time, allowing for some decrease in SNR, as in (c). All images are produced from acquisitions using fully sampled data.

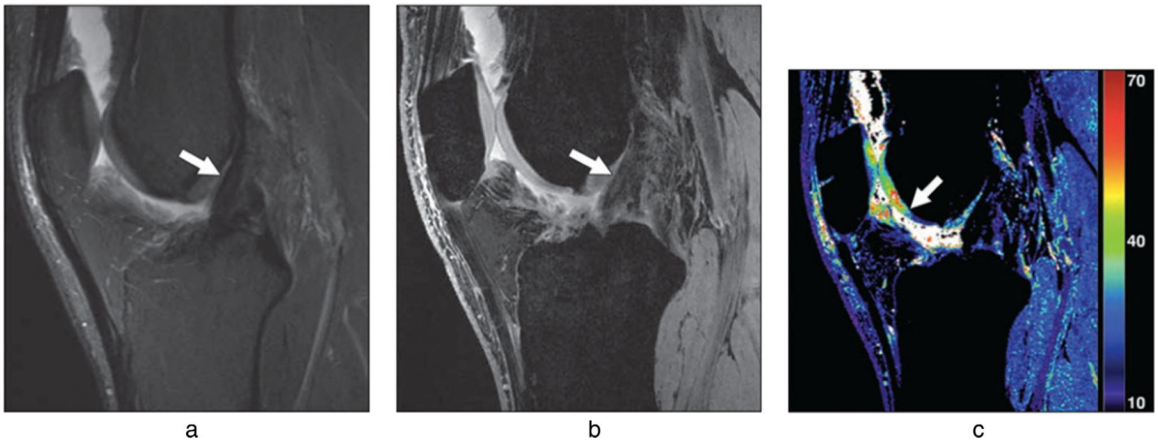

FIGURE 7:

(a) Sagittal T_2-weighted MR image shows an intact anterior cruciate ligament (ACL) graft with conspicuity (arrow), (b) quantitative double-echo steady-state (qDESS) MR image with mixed T_2- and T_1-weighted echo shows conspicuity of the anterior cruciate ligament graft (arrow) similar to (a), (c) qDESS T_2 map (values in milliseconds) shows focal increased T_2 relaxation time (arrow) of the trochlear cartilage despite morphologically normal cartilage identified in (a) and (b).[60] *Source*: Images courtesy of Dr. Akshay Chaudhari, PhD, Stanford University, USA.

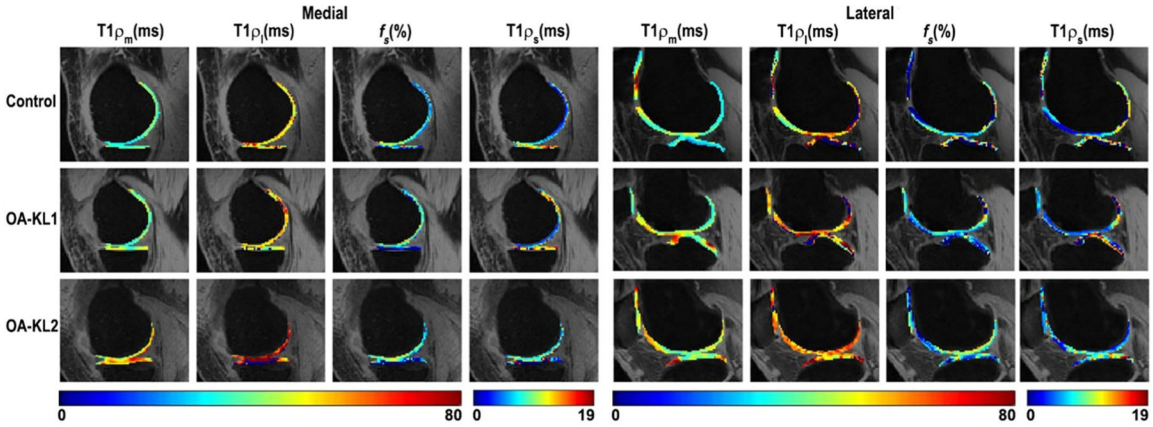

FIGURE 8:

Representative examples of multicomponent $T_{1\rho}$ results of the knee cartilage, from age-matched (55 ± 2 years old) healthy control and early OA patients (KL-1,2). Maps refer to mono-exponential $T_{1\rho}$ ($T1\rho_m$), bi-exponential long $T_{1\rho}$ component ($T1\rho_l$), bi-exponential short $T_{1\rho}$ component ($T1\rho_s$), and bi-exponential fraction of the short component (f_s). Left panel: medial cartilage and Right panel: lateral cartilage. *Source*: Unpublished data, courtesy of Dr. Ravinder Regatte, PhD, New York University, USA.

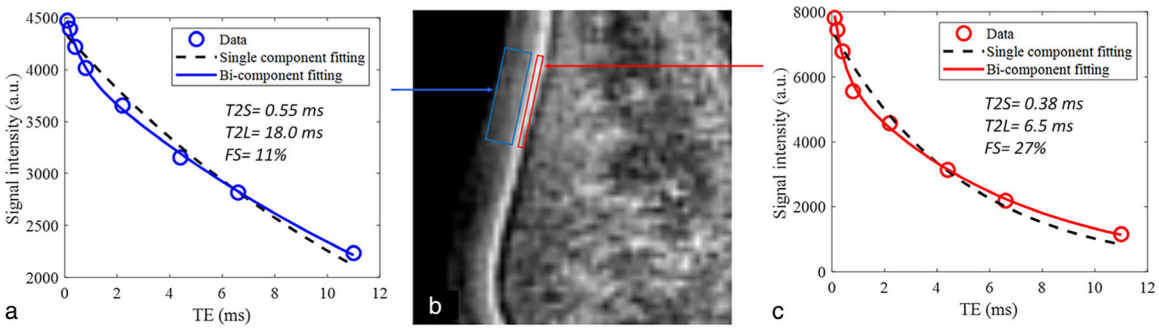

FIGURE 9:

Mono and bi-exponential T_{2*} analysis of the knee cartilage. (a) For the more superficial cartilage region, the T_{2*} values of short and long components as well as the short fraction were 0.55 msec, 18.0 msec, and 11.0%, respectively. (c) For the deeper cartilage region, the values were 0.38 msec, 6.5 msec, and 27.0%, respectively. Regions marked in (b). *Source*: Images courtesy of Dr. Jiang Du, PhD, University of California at San Diego, USA.

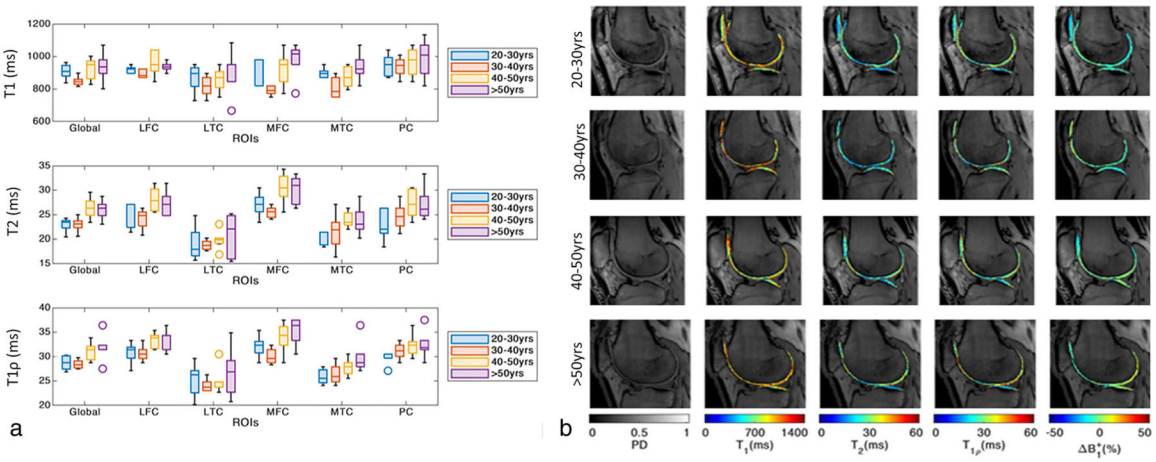

FIGURE 10:

(a) Boxplot of cartilage T_1, T_2, and $T_{1\rho}$ values for the different age groups, (b) illustrative cartilage proton density (PD), T_1, T_2, and $T_{1\rho}$ maps of the lateral cartilage.[89] LFC-lateral femoral cartilage, LTC lateral tibial cartilage, MFC-medial femoral cartilage, MTC-medial tibial cartilage, PC-patellar cartilage.

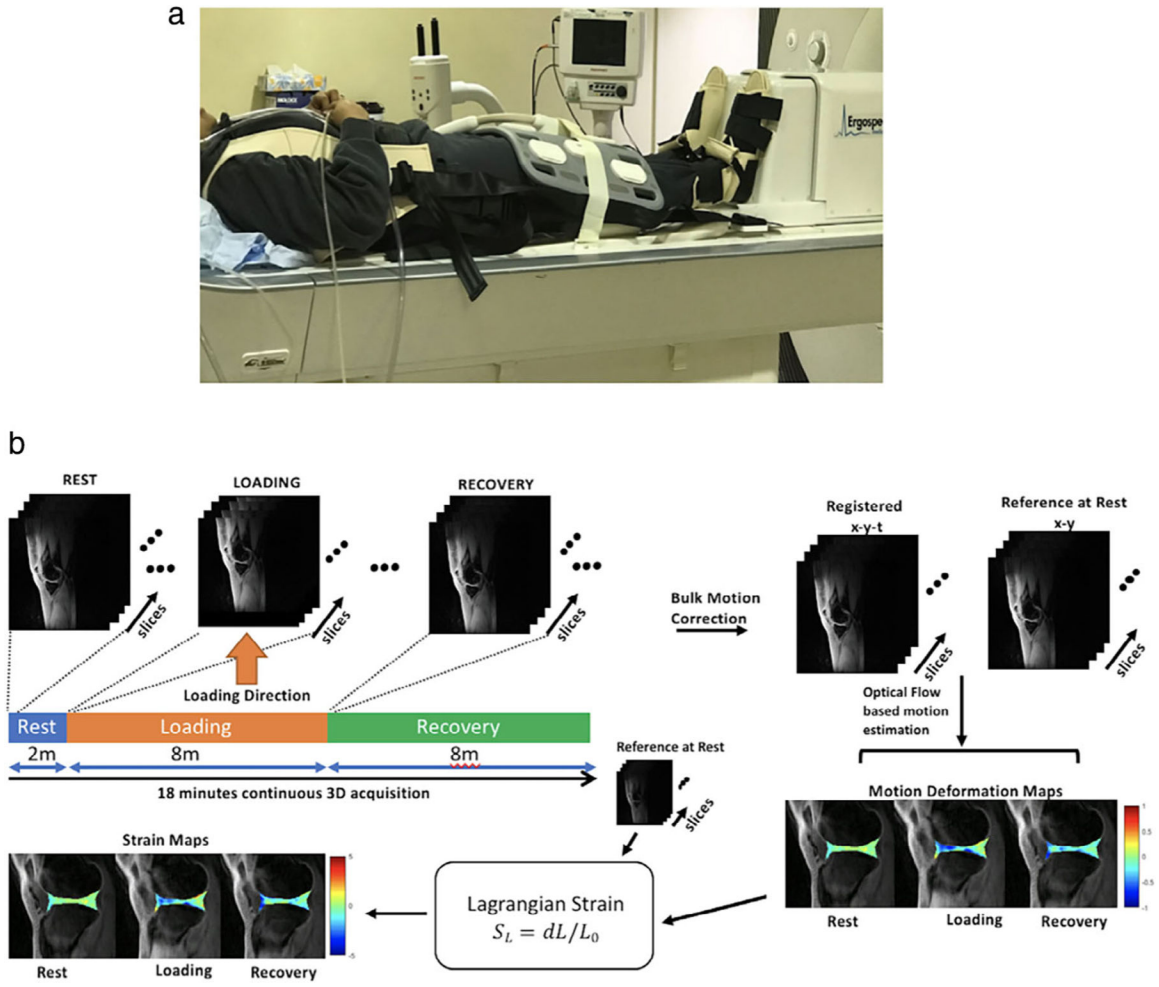

FIGURE 11:

(a) A photograph of the experimental setup used to asses cartilage strain maps under mechanical loading during MRI scan.[99] (b) Illustration of the process, consisting of an 18 minutes continuous acquisition using golden-angle radial acquisitions while the knee joint at rest, during mechanical loading, and during recovery. The image reconstruction is performed with compressed sensing methods, followed by motion correction using optical flow methods, and finally, Lagrangian strain is calculated to produce cartilage strain maps.

TABLE 1.

Summary of Current State-of-The-Art Techniques Used for Cartilage Compositional MRI

MRI Method	Measurement	Interpretation
T_2 Mapping	Water, collagen structure	T_2 increase signifies the breakdown of the organized collagen structure
T_{2*} Mapping	Water, collagen structure and local magnetic field inhomogeneity	T_{2*} increase signifies the breakdown of the organized collagen structure and local magnetic field inhomogeneity
$T_{1\rho}$ Mapping	GAG	$T_{1\rho}$ increase signifies GAG depletion
T_1 Mapping/dGEMRIC	GAG	T_1 decrease signifies GAG depletion
UTE MRI	Short T_2 components	Provides signal from tightly bound water in collagen-rich tissues
gagCEST MRI	Water and GAG	gagCEST decrease signifies GAG depletion and it is specific to GAG
Sodium MRI	GAG	Sodium signal decrease signifies GAG depletion and it is specific to FCD
Diffusion MRI	Water and PG/collagen	ADC signifies PG depletion FA correlates with collagen structure
Morphometry	Cartilage thickness, volume, and area	Reduction of these morphological measurements corresponds to loss of cartilage